Laser Raster Conditioning of KDP and DKDP Crystals using XeCl and ND:YAG Lasers

M. Staggs, M. Yan, and M. Runkel

U.S. Department of Energy

Lawrence
Livermore
National
Laboratory

December 20, 2000

DISCLAIMER

This document was prepared as an account of work sponsored by an agency of the United States Government. Neither the United States Government nor the University of California nor any of their employees, makes any warranty, express or implied, or assumes any legal liability or responsibility for the accuracy, completeness, or usefulness of any information, apparatus, product, or process disclosed, or represents that its use would not infringe privately owned rights. Reference herein to any specific commercial product, process, or service by trade name, trademark, manufacturer, or otherwise, does not necessarily constitute or imply its endorsement, recommendation, or favoring by the United States Government or the University of California. The views and opinions of authors expressed herein do not necessarily state or reflect those of the United States Government or the University of California, and shall not be used for advertising or product endorsement purposes.

This is a preprint of a paper intended for publication in a journal or proceedings. Since changes may be made before publication, this preprint is made available with the understanding that it will not be cited or reproduced without the permission of the author.

Laser Raster Conditioning of KDP and DKDP Crystals using XeCl and ND:YAG Lasers

Mike Staggs, Ming Yan and Mike Runkel

Lawrence Livermore National Laboratory, PO Box 808, L-411, Livermore, CA 94551

ABSTRACT

Laser conditioning by raster scanning KDP and DKDP crystals using Nd:YAG and XeCl excimer laser systems was demonstrated. The laser systems were evaluated to determine their respective feasibility of improving the damage thresholds of the harmonic materials for use on the National Ignition Facility (NIF). Crystals were first evaluated using an Nd:YAG laser (355 nm, 7.6 ns) by scanning 2 x 2 cm^2 areas with sub-damage threshold fluences and then performing unconditioned (S/1) damage tests at 355-nm in the respectively scanned regions. Subsequently, five KDP and DKDP samples of various damage quality were raster scanned in a similar fashion at MicroLas GmbH (Goettingen, Germany) using a commercial Lambda Physik Excimer system (XeCl, λ = 308 nm, 20 ns). The samples treated in Germany were then tested at Livermore National Laboratory (LLNL) at 355 nm to demonstrate the excimer's potential as an alternative conditioning source.

The excimer scan results suggest that crystals can be treated at high fluence (50 J/cm2, 308-nm, 20-ns) levels without noticeable bulk damage. In addition, comparable conditioning is possible even with the fluence set at 30% of the 308-nm damage threshold. The laser damage tests with 355-nm on the majority of the excimer laser-treated crystals demonstrates the effect of conditioning, by raising the S/1 threshold or by reducing the low fluence tail of the 355-nm S/1 damage probability curves. Furthermore, the high average power and flat top beam profile of an excimer laser makes it possible to laser condition a 42-cm NIF-size crystal in one day, compared to 41 days for a commercial table-top Nd:YAG system. The test samples were to be particularly susceptible to surface damage during excimer raster conditioning, possibly due to high levels of dust and/or contaminants in the laboratory environment.

Keywords: KDP, DKDP, laser damage, laser conditioning, S/1, N/1, R/1

1. INTRODUCTION

Potassium dihydrogen phosphate (KDP) and deuterated potassium dihydrogen phosphate (DKDP) are widely used to generate harmonics of laser frequencies. Systems employing these materials include small table-top commercial lasers and large lasers for inertial confinement research such as the National Ignition Facility (NIF) currently in production at LLNL. Researchers at LLNL and others have observed that KDP, its isomorphs, and other wide band-gap materials, limit usable beam fluences due to the occurrence of bulk damage.[1-6] Two classes of damage mechanisms have been studied to explain the resultant bulk damage in these materials. The first is the extensively studied breakdown of defect-free pure materials.[7,8] The second involves studies in understanding chemical, structural, and/or mechanical defect contributions to the initiation and growth of laser induced damage. Currently, electric field enhancement and localized absorption have been identified as the most likely cause of the observed bulk damage.[9,10] Although the exact mechanism or mechanisms responsible for the observed bulk damage has not been identified, results have demonstrated that the bulk damage threshold of KDP and DKDP crystals can be increased by a factor of 1.5 to 2 through Nd:YAG 355-nm laser conditioning (i.e., a process of raising the damage threshold of a material by irradiating the material at sub-threshold fluences).[11,12] In addition, the excimer 308-nm effect on 1.064-µm operation of KDP was explored by Gong et. al., Boulder Damage Symposium, 1998.[13]

*Correspondence: Email: Staggs3@llnl.gov Telephone: 925 422 3682; Fax: 925 422 3611

To date, all NIF-scale (42-cm) DKDP crystals produced by both rapid and conventional growth techniques require laser conditioning to meet the obscuration specification of 0.1% for operation at full fluence (8 J/cm^2 average, 351 nm, and 3 ns).[14] While the crystals initially installed may be conditioned on-line by gradual increases in beam energy, subsequent crystals must be conditioned off-line to maximize the use of the National Ignition Facility. The most feasible approach is raster-scanning the triplers using a UV laser system. This work demonstrates that raster scanning with a frequency tripled Nd:YAG can increase the damage resistance of KDP and DKDP so that the S/1 (i.e., unconditioned damage test using the same fluence, n number of pulses at a single site) damage distribution moves to near the R/1 (i.e., conditioning damage test using a slow ramp fluence increase, n number of pulses at a single site but n not always the same for each site) damage probability distribution. As a means of reducing the scan time for a 42-cm NIF tripler, we also investigated raster-conditioning using an excimer laser (308-nm, 20-ns). The high output power and flat top spatial beam profile of such a system allow large spot sizes with the required fluences. An excimer laser system can thus reduce the time for raster scanning a 42-cm NIF size harmonic conversion crystal to within one day.

2. EXPERIMENTAL SET-UP

Figure 1 shows the 355-nm Zeus[15] raster damage test system layout. The laser source is a commercially available Spectra-Physics Nd:YAG operating at 10Hz with a 7.6-ns temporal pulse-width. The energy is focused to a far-field diffraction limited spot size in the sample plane with a Rayleigh range that allows the entire thickness of the sample to be irradiated with a constant fluence. A CCD coupled with a Helium-Neon source act as a scattering diagnostic to detect the onset of bulk damage. Raster conditioning was accomplished by scanning the sample continuously in a horizontal direction from one end of the crystal to the other and then stepping vertically at the end of each scan as shown at the bottom right of Fig.1. During raster scanning, the successive laser pulses overlap spatially to achieve uniform conditioning over the entire crystal. For the Nd:YAG tests (355-nm, 7.6-ns, 1-mm FW at 1/e^2), the scan rate was set so that 20 laser shots overlap within 200-μm, which is the laser beam-width at 90% of the peak intensity.
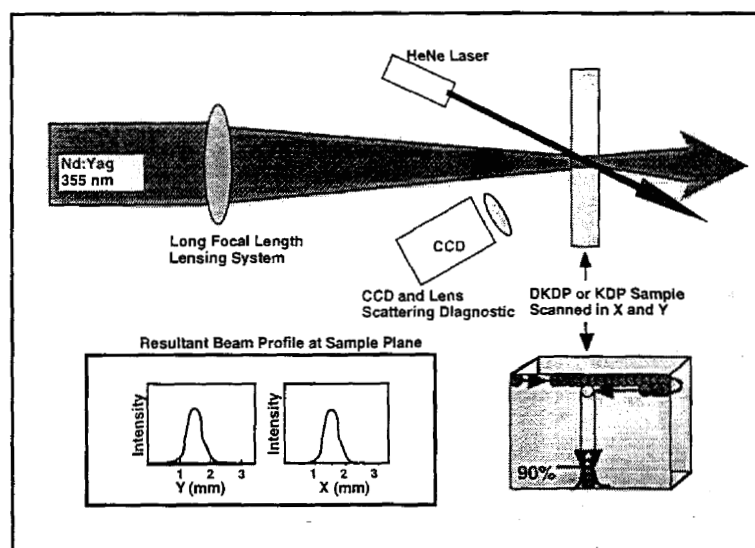

Figure 1. Optical layout of the Nd:YAG laser conditioning system, which consists of a long focusing lens, diagnostics, and x-y raster scanning capabilities. The lower left shows the resultant YAG beam profiles with an approximately 1-mm FW spot size at 1/e^2 in the x and y axis.

Figure 2 shows the 308-nm raster damage test system layout. The laser source here is a commercially available, high-average-power (120W) Lambda Physik excimer (XeCl), which can operate up to 100Hz with a 20-ns temporal pulse-width. The output laser beam is imaged through a homogenizer, that consists of a single array of cylindrical lenses, and is subsequently focused to achieve high laser fluences. Damage diagnostics were similar to the aforementioned YAG system. The spatial beam profile at the sample is shown at the bottom left of fig.2, and exhibits the flat top profile along the long axis (y) and a semi-gaussian profile along the short axis (x). The image blur length at focus is approximately 3-5-cm. In the raster scanning process, the sample was scanned continuously

along the x-axis and then stepped along the y-axis at the end of each scan. The semi-gaussian beam cross-section in the scanning direction allows the utilization of the low fluence wings for ramping up the local fluence at a fixed sample site during raster scanning. The flat-top beam cross-section in the long axis allows rapid stepping perpendicular to the scanning direction. The flat top beam profile utilizes the total energy of the laser pulse most efficiently and yields the lowest scan times, since the degree of conditioning is mainly determined by the peak fluence of the laser pulse. The scanning speed was set so that the top 90% of the gaussian beam in the x-axis overlaps in 20 laser shots. With the spatial beam profile as shown in Fig. 2, the maximum fluence at the sample position is about 50 J/cm^2 with a laser output energy of 360 mJ per pulse. Thus, it is feasible to use an excimer to scan a NIF-size DKDP crystal within one day.
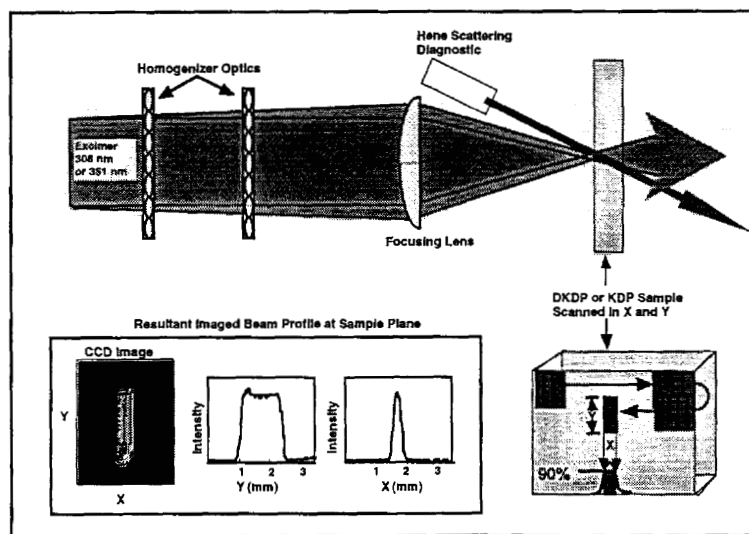

Figure 2. The optical layout of the excimer laser conditioning system, which consists of a homogenizer, focusing lens, and raster scanning capabilities. The lower left shows the resultant excimer beam profiles as captured on a CCD. The long axis (y) exhibits a flat top beam profile while the short axis (x) is a quasi-gaussian.

3. RESULTS

3.1 Nd:YAG Scanning Results

Figure 3 shows the laser-induced damage probability before and after raster conditioning using an Nd:YAG (355-nm,7.6-ns) laser system for z-cut crystal samples KDP 347 and KDP 214. These crystals were high damage threshold crystals, which represent goals for NIF production. It appears that the S/1 (unconditioned) thresholds of both crystals are improved after laser raster scanning. The data suggests that by raster scanning with sub-damage threshold laser pulses, an increase of the laser damage resistance to the level of the ultimate conditioned threshold (i.e. R/1 threshold) is obtainable. It is also important to note that the degree of improvement depends on the laser fluence used for the conditioning process. Figures 3(a) and 3(b) show the effect of different laser fluences for conditioning. Crystal 347 has been raster conditioned at 15 J/cm^2 as indicated by the vertical bar in Fig. 3(a). Crystal 214c, shown in fig. 3(b), has been raster conditioned with two successive fluences, 8 J/cm^2 and 14 J/cm^2, as indicated by the two vertical bars that intersect its corresponding fluence scale on the x-axis of figure 3(b). The second fluence used for crystal 214c is much closer to the low fluence tail of the R/1 curve than the fluence used for crystal 347 as seen in Fig. 3(a). In crystal 214c-2, the S/1 threshold after raster conditioning is close to its measured R/1 threshold. Meanwhile, only the low fluence tail of the S/1 curve is reduced after raster conditioning crystal 347. This may be because the final raster scan of crystal 214c was at a fluence close to the tail of its measured R/1 curve, while the final and only scan of crystal 347 was still somewhat below the tail of its R/1 measured curve. Thus, it appears that maximum conditioning requires the use of the highest possible laser fluence. However, conditioning is limited by the risk of laser damage, which is determined by the low fluence tail of the R/1 damage probability curve.

This result suggests that laser conditioning is a process that strongly relates to the mechanism of laser damage. We speculate that conditioning is a process of a local modification of crystal properties by local heating, which causes diffusion of absorbing defects (e.g., metal phosphate nano-particles) whose absorption is sufficiently high to cause damage. We believe that local laser irradiation facilitates the process of diffusion of such absorbing particles. A slight difference in laser fluence near the damage threshold will result in either diffusion (conditioning) or breakdown (damage) of the local absorbing materials.
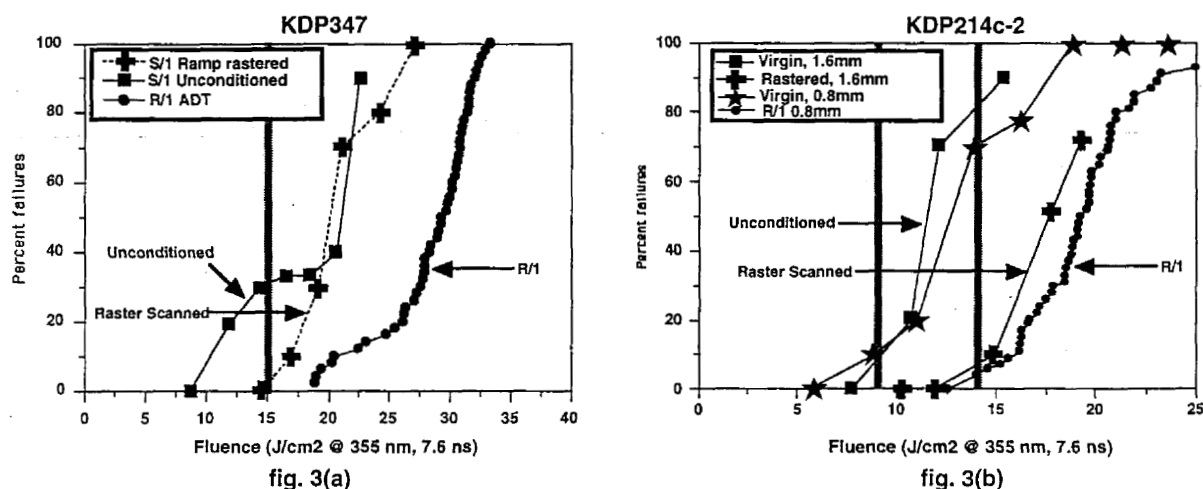

fig. 3(a)

fig. 3(b)

Figure 3. a) Depicts how a one-step raster conditioning (15 J/cm^2 as shown by the vertical bar) process can remove the low fluence tail of the S/1 curve for crystal 347. b) Shows how a two step raster conditioning process (8 and 14J/cm^2 as shown by the vertical bars respectively) can improve the S/1 threshold up to the tail of the R/1 curve of crystal 214c-2.

Even though raster scanning at 355-nm has been successful in laser conditioning of KDP crystals, it is impractical to use a Nd:YAG laser to condition a 41x41-cm^2. We estimate that it will take about 41 days to condition a 40-cm crystal using a YAG laser with a 0.5 J per pulse at 10Hz to reach a laser fluence of 23 J/cm^2 (assuming that our $t^{0.5}$ scaling law is correct).

3.2 Excimer Scanning Results

Using the above mentioned excimer laser system at MicroLas Lasersystem, we laser conditioned six z-cut samples listed in Table 1. These samples were specifically chosen to cover a wide range of crystal parameters, enabling us to evaluate the effectiveness of conditioning large areas of potential NIF materials at the 308-nm wavelength.

Table 1. Description of samples tested for laser conditioning using an excimer laser at 308 nm.

Sample ID	Specification
LL3	high threshold, (70% deuterated DKDP), conventional growth
DKDP 586	high threshold, rapid growth DKDP
LL1	low threshold, (80% deuterated DKDP), conventional growth
RG8A	low threshold rapid growth DKDP sample from a large boule
335	rapid growth DKDP sample from a small boule
KDP214	rapid growth KDP sample from a clean salt (pyramidal cap)

First, we experimentally determined the N/1 (conditioned) damage threshold at 308-nm with a pulse width of 20 ns. Given a clean area, we could ramp-up the fluence in discrete steps to the limit of the laser's capabilities (~50 J/cm^2, 20 ns) in all the test samples without bulk damage. Using the t$^{0.5}$ temporal pulse width scaling, the damage threshold of 50 J/cm^2 at 20 ns is equivalent to 32 J/cm^2 at 7.6 ns, which is higher than the R/1 damage probability at 355 nm for those crystals. This result implies that either the laser damage threshold at 308 nm is higher than at 355 nm, or that 308-nm radiation is better for conditioning than 355-nm. The first conclusion is unlikely since the damage threshold typically decreases as the wavelength becomes shorter. We believe that 308-nm radiation might be more efficient for laser conditioning since 308 nm light is more highly absorbed by those defects.

It was not possible to determine the N/1 damage threshold at 308 nm over large areas because of frequent surface damage caused by surface contamination and/or dust particulates in the air. The observed damage correlated with visible dust particulates landing on the surface or other pre-existing surface contamination. Most of the samples used in these tests were either finished at a considerably earlier date, or had previously been damage tested. Due to the surface damage by contamination, every sample was raster scanned over an approximate area of 1.5 x 1.5 cm area with a fluence of ~ 14 J/cm^2, which corresponds to only one-third of the 20-ns damage threshold at clean spots.

Figure 4 shows the results of an initial N/1 test on sample 214c-3. The right axis in Fig. 4 corresponds to the initial R/1 curve given for sample 214. The left axis is showing each discreet fluence step increase (22 steps total, each bar represents 100 pulses at 100Hz) culminating in a final fluence of 50 J/cm^2 using 308-nm, 20-ns. To illustrate how we can achieve an equal or greater conditioning effect at 308 nm than at 355 nm using an Nd;YAG system, the bars are plotted to the scaled 7.6-ns x-axis using t$^{0.5}$ as the scaling law.
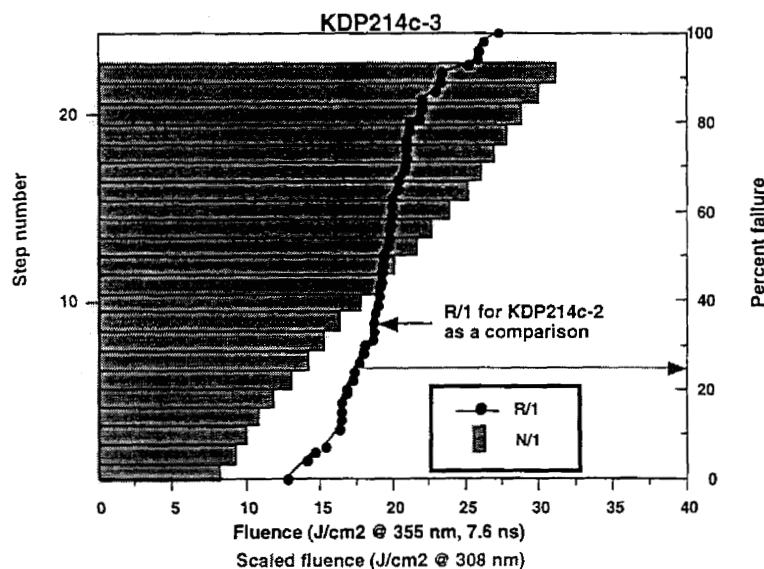

Figure 4. Initial demonstration of N/1 conditioning on KDP214c-3. Each grey bar represents an excimer N/1 test (100 pulses at 100Hz, 308 nm, 20 ns) and corresponds to the left axis which depicts the step number (i.e., discreet increase in fluence). The right axis depicts the % failure (i.e., R/1 damage probability) and relates to the blue curve as tested previously at Livermore using an Nd:YAG system (355 nm, 7.6 ns). The excimer fluence was scaled to 7.6 ns using t$^{0.5}$.

Figure 5 shows how low-fluence 308-nm conditioning increases the S/1 damage probability at 355 nm for samples RG8A and LL1-51. RG8A (fig. 5(a)), was a valuable calibration sample due to its low R/1 and S/1 thresholds at 7.6 ns. Because of its poor damage quality, we were able to obtain very prominent visible bulk damage with single pulses at 14 J/cm^2 with the excimer laser. We then demonstrated the conditioning of crystal RG8A with an 8-step sequence culminating in the scanning fluence of 14 J/cm^2 at a laser repetition rate of 10Hz. After raster conditioning the KDP crystal, the sample was refinished by diamond turning and laser damage tested at 355 nm, 7.6-ns to determine the S/1 damage threshold in unconditioned and raster-conditioned areas. Figure 5(a) shows that the S/1 damage threshold in the 308-nm irradiated area occurs at higher fluences relative to the virgin area. As shown in

Figure 5(b), sample LL1-51 also has a low S/1 damage threshold but with a long, low-fluence tail represented in its R/1 damage probability curve (from LL1-53). This crystal was raster conditioned using a laser fluence of 14 J/cm² at a 10Hz repetition rate. The S/1 damage probability after raster conditioning as seen in fig. 5(b) shifts to higher fluences relative to the unconditioned S/1 curve. Assuming that the R/1 thresholds of LL1-51 and LL1-53 are the same, the damage after raster conditioning is still dominated by defects that cause the low fluence tail of the R/1 curve. It is notable that the low fluence foot of the S/1 curve after 308-nm irradiation is higher than that of the R/1 curve. Since we believe that R/1 represents the ultimate conditioning by 355-nm laser pulses, this result suggests that raster conditioning using 308-nm light possibly might reduce the low fluence tail more efficiently than at 355 nm. This observation needs to be explored further using a higher fluence at 308 nm for raster conditioning once the surface damage problem is overcome.
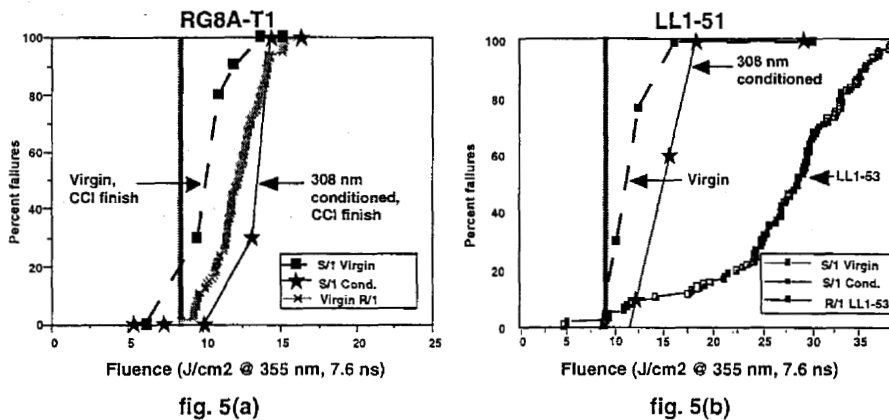

fig. 5(a)   fig. 5(b)

Figure 5. a) The damage probability curves for S/1 unconditioned (virgin), S/1 308-nm conditioned and, R/1 for sample RG8A. The solid vertical bar represents the equivalent fluence used for conditioning and is scaled to 7.6-ns by $t^{0.5}$. b) The S/1 damage probability of crystal LL1-51 before and after excimer laser conditioning. The R/1 damage threshold of LL1-53 is plotted for comparison. The solid vertical bar indicates the 308-nm fluence used for conditioning and is scaled to 7.6-ns by $t^{0.5}$.

Crystals 335, LL3-51, and DKDP 586 evinced a different result from samples RG8A and LL1-51, as shown in figures 6(a), 6(b), and 6(c) respectively. All three samples were raster conditioned at 14 J/cm² and all three samples appear to show a similar reduction of the low fluence tail of their S/1 curves. For DKDP 586 as shown in fig. 6(c), an additional test was constructed in which five virgin sites were exposed to ten pulses of 308-nm at approximately 50 J/cm², resulting in three of the sites having large amounts of bulk damage. We then targeted six sites within the raster-conditioned area using ten pulses of 50 J/cm² with no damage visible with our diagnostics. This demonstrates the conditioning effect of 308 nm, suggesting we may be able to: 1) condition at a much lower fluence, and 2) still achieve the desired results using 308 nm.
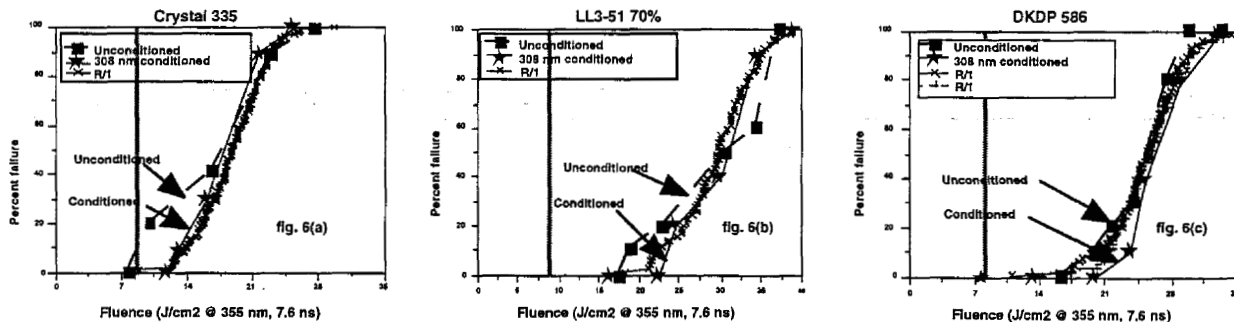

Figure 6. a) The S/1 damage probability of crystal 335 before and after excimer laser irradiation. b) The S/1 damage probability of crystal LL3-51 before and after excimer laser irradiation. c) The S/1 damage probability of crystal DKDP 586 before and after excimer laser irradiation. The red bar in all three plots indicates the 308-nm fluence used for conditioning and is scaled to 7.6 ns by $t^{0.5}$.

Finally, a comparison between Nd:YAG laser conditioning and excimer conditioning can be seen by the results of KDP 214 as shown in fig. 7. This sample was the first rapidly grown high damage threshold crystal grown at LLNL using continuous filtration and high purity starting material from a pyramidal cap. Figure 7 shows the unconditioned, and 308-nm and 355-nm raster-conditioned S/1 threshold material for two different samples from the same boule. Even though the two unconditioned S/1 damage curves have a shift for which the cause is currently unknown, the relative increase of the S/1 curve after laser conditioning by 308 nm and 355 nm is almost the same in both cases.
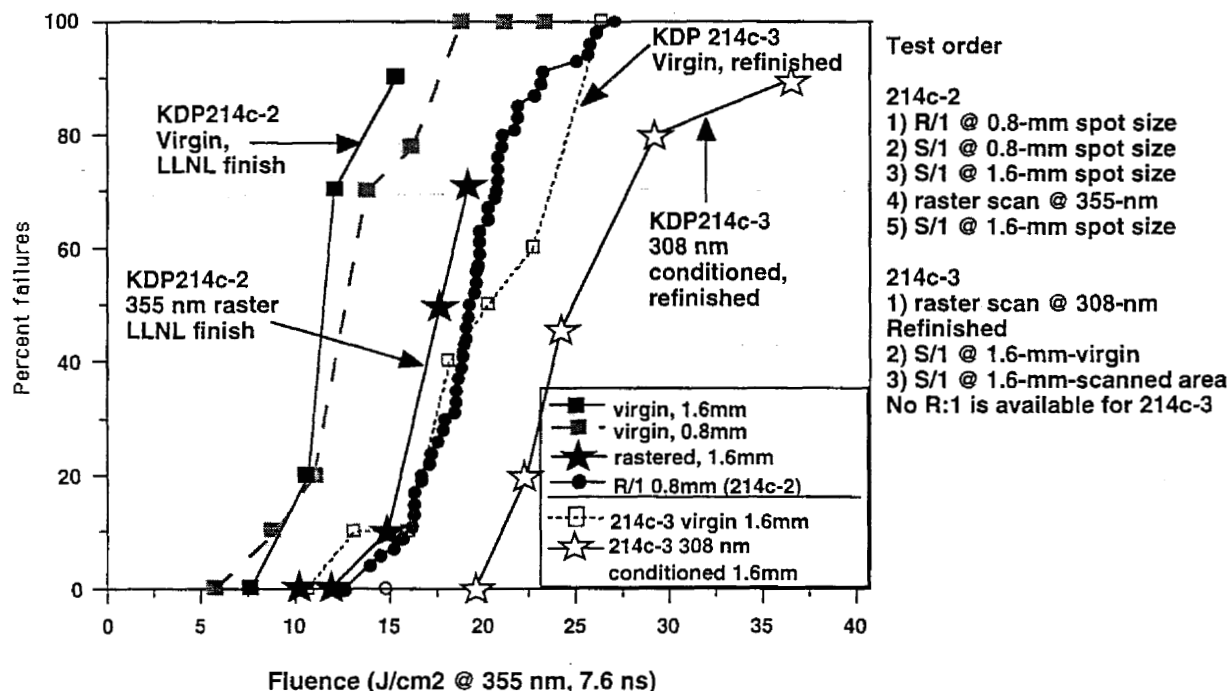

Figure 7. The S/1 damage probability curve of two samples from KDP 214 boule. KDP 214c-2 was raster conditioned with an Nd:YAG laser at 355 nm and KDP 214c-3 was conditioned with an XeCl excimer laser at 308 nm. The relative fluence shift due to conditioning is about the same, but the 308-nm fluence used for conditioning is relatively low.

4. CONCLUSION.

This work demonstrates for the first time that using a table-top Nd:YAG laser, we can raster-condition KDP and DKDP crystals resulting in an improvement in their S/1 damage probability distribution. In addition, this is the first experimental demonstration of laser conditioning DKDP and KDP crystals using an excimer laser source. The crystals can be treated at high fluence levels at single sites with a 308-nm laser without noticeable bulk damage. It has been shown to be effective at conditioning even with the fluence set at 30% of the damage threshold at 308 nm. Laser damage tests with 355 nm on most of the excimer laser treated crystals demonstrates the effect of conditioning on the S/1 threshold at 355 nm. The high average power and flat top beam profile makes it possible to laser condition a 42-cm crystal within a day. Additional tests are planned to further quantify the excimer conditioning and surface damage effects on state-of-the-art, large-boule rapid and conventional growth crystals.

ACKNOWLEDGEMENT

REFERENCES

1. I.A. Batyreva, V. I. Bespalov, A. M. Kiselev, and A.M. Miller, "Characteristics of laser pulse damage to water-soluble non-linear crystals," Sov. J. Quantum Electron, Vol.8, pp. 1044-1046, 1978.

2. R. M. Wood, "Laser Damage in Optical Materials at 1.06μ," GEC J. Science Technol. Vol. 45, pp. 109-115, 1979.

3. J. Swain, S. Stokowski, D. Milam, and Frank Rainer, "Improving the bulk laser damage resistance of potassium dihydrogen phosphate crystals by pulsed laser irradiation," Appl. Phys. Lett., Vol. 40, pp. 350-352, 1982.

4. S. C. Jones, P. Braunlich, R. T. Casper, X. A. Shen, "Recent progress on laser-induced modifications and intrinsic bulk damage of wide-gap optical matrials," , Optic. Engin., Vol. 28, pp. 1039-1067, 1989.

5. B. C. Stuart, M. D. Feit, A. M. Rubenchik, B. W. Shore and M. D. Perry, "Nanosecond-to-femtosecond laser induced breakdown in dielectrics," Phys. Rev. B, Vol. 53, pp. 1749-1761, 1996.

6. P. Braunlich, S. C. Jones, X. A. Shen, and R. T. Casper, "Laser-induced modifications and the mechanism of intrinsic damage in wide-gap optical materials," Nuclear Instruments & Methods In Physics Research Section B,Vol. 46, pp. 224, 1990

7. 1 N. Bloembergen, "Laser induced electric breakdown in solids," IEEE J. of Quantum Electr., 10, pp. 375-386, 1974.

8. W. L. Smith, "Laser induced breakdown in optical materials," Optic. Engin., Vol. 17, pp. 489-583, 1978.

9. E. S. Bliss, "Laser-damage mechanisms in transparent dielectrics", Damage in laser glass, ASTM STP vol. 469, pp. 9-20, 1969.

10. L.L. Chase, "Laser Ablation and optical surface damage," Springer Series in Material Science, J. C. Miller, Ed., Springer-Verlag, Berlin, Vol. 28, pp. 53-82., 1994.

11. L.J. Atherton, F. Rainer, J.J. De Yoreo, I.M. Thomas, N. Zaitseva and F. De Marco, "Thermal and Laser conditioning of production and rapid-growth KDP and KD*P crystals," In Laser Induced Damage in Optical Materials, SPIE Proceedings, Vol. 2114, pp. 36-45, 1993.

12. M. Runkel, J.J. DeYoreo, W.D. Sell, D. Milam, "Laser conditioning study of KDP on the optical sciences laser using large area beams," In Laser Induced Damage in Optical Materials, Vol. 3244, pp.51-63, 1997.

13. H. Gong, Y. Sun, C. Li, " Effects of excimer laser irradiation on the KDP crystal," In Laser Induced Damage in Optical Materials, SPIE Proceedings, Vol. 3578, pp. 516-518, 1998.

14. M. Runkel, W. Williams, J. De Yoreo, "Predicting bulk damage in NIF triple harmonic generators," In Laser Induced Damage in Optical Materials," SPIE Proceedings, Vol. 3578, pp. 322-331, 1998.

15. M. Runkel, M.Yang, J. De Yoreo and N. Zaitseva, "The effect of impurities and stress on the damage distributions of rapidly grown KDP crystals," In Laser Induced Damage in Optical Materials, SPIE Proceedings, Vol. 3244, pp. 211-222, 1997.